Journal of Cleaner Production 170 (2018) 278–287

Contents lists available at ScienceDirect

Journal of Cleaner Production

journal homepage: www.elsevier.com/locate/jclepro

Characterization and modelling optimization on methanation activity using Box-Behnken design through cerium doped catalysts

Salmiah Jamal Mat Rosid, Wan Azelee Wan Abu Bakar*, Rusmidah Ali

Department of Chemistry, Faculty of Science, Universiti Teknologi Malaysia (UTM), 81310, Skudai, Johor, Malaysia

ARTICLE INFO

Article history:
Received 15 May 2017
Received in revised form
7 September 2017
Accepted 7 September 2017
Available online 8 September 2017

Keywords:
CO_2
Methanation
Response surface methodology
Box-Behnken design
Cerium oxide

ABSTRACT

Catalytic methanation reaction has been a promising technique for the conversion of CO_2 to valuable fuel product, CH_4 and thus reduces the emission of CO_2 to the environment. Many catalysts have been investigated by this method yet some carbon depositions have occurred during reaction which leading to low conversion rate of CO_2 to CH_4. Therefore, cerium catalyst has been applied in this study for the investigation of catalytic activity utilizing response surface methodology (RSM) method (Box-Behnken Design) in order to achieve the highest CO_2 conversion. The potential trimetallic oxide catalyst of Ru/Mn/Ce (5:35:60)/Al_2O_3 was chosen and the experimental parameters used were calcination temperature of 600–800 °C, ratio based loadings of 60–80 wt%, and catalyst dosage of 3–7 g with CO_2 conversion to CH_4 as a respond. The RSM optimum parameter of calcination temperature of 697.47 °C, ratio of 60.38% and catalyst dosage 6.94 g was tested. At these conditions, the results were verified experimentally (99.98% CO_2 conversion), which was accurately close to the predicted value (100% CO_2 conversion). Ru/Mn/Ce (5:35:60)/Al_2O_3 catalyst revealed the active species of CeO_2 in XRD analysis with oxidation state Ce^{4+} as supported by ESR analysis. When the calcination temperature was increased, the surface area decreases as observed in nitrogen adsorption supported with larger particle size as shown in FESEM. The reducibility of cerium catalyst was started at lower temperature.

1. Introduction

Natural gas has received a great demand for the industry and daily activities which at the same time to achieve a reduction of greenhouse gases [Pan et al., 2017, Osazuwa and Cheng, 2017]. However, Malaysia's natural gas producing sour natural gas which consists of polluted gaseous such as CO_2 which accumulate in the atmosphere when it was released to the environment [Pan et al., 2017]. Therefore, green technology is necessary to identify and solve the issues of energy and environmental gradually for all over the world as stated by Islam et al (2009).

Thus, to produce a clean burning and environmental friendly of natural gas [Dong et al., 2017, Kakaee et al., 2014], a gas sweetening process is needed to remove of acid gases such as CO_2, H_2S and other sulphur components [Zhang et al., 2017, Sadegh et al., 2017]. The most promising method for removing higher content of CO_2 from natural gas is catalytic methanation. This methanation process has been widely explored in terms of catalysts and condition processes. For the natural gas purification, the important process is conversion of carbon dioxide to methane by using hydrogen gas as shown in Equation (1.1) below [Toemen et al., 2017].

$$CO_2 + 4H_2 \xrightarrow{\text{Catalyst}} CH_4 + 2H_2O \quad (1.1)$$

The most important criteria for the methanation catalyst are thermal stability, coke formation, fouling, and basicity. Thermal stability is an important to make sure that the reaction temperature is low because it affects the equilibrium state of the reaction and the catalyst life decreases if it is too high. The formation of coke will blocks the reactants from reaching the active site and the fouling are formed by the reaction forming a product which when covered on the active site. Besides that, the catalyst selection for CO_2 methanation reaction should have higher basicity and high surface area with small particle sizes dispersed on the catalyst surface. The dispersion may help to stabilize the active species [Toemen et al., 2017].

However among other catalysts studied, the deactivation of catalyst always occurs due to carbon deposition on the catalyst surface. Therefore, it is necessary to develop catalysts that are

* Corresponding author.
E-mail address: wazelee@kimia.fs.utm.my (W.A. Wan Abu Bakar).

https://doi.org/10.1016/j.jclepro.2017.09.073
0959-6526/

highly efficient and stable against sintering and carbon deposition. Up to date, only a few researchers have investigated the lanthanide oxide as based catalyst towards methanation reaction. Based on the Du et al., 2007 studies, the using of lanthanide elements can affect the physical and chemical characteristic of the based catalyst. One of the elements that have been investigated was cerium. This is due to its high specific surface area and strong redox ability. It also possesses a higher degree of stabilization upon ionization [Biinzli and Piguet, 2005]. Rao and Mishra, 2003 also stated that a highly basic catalyst like cerium oxide can enhance the CO_2 adsorption and chemisorption on the catalyst surface. Its excellent redox properties resulted in a very fast reduction of Ce^{4+}/Ce^{3+}, which attributed to the formation of oxygen vacancies on the surface.

Rynkowski et al. (2000) had investigated the activity of Ru/Al_2O_3 and $Ru/CeO_2/Al_2O_3$ catalysts for methanation reaction with 72% and 76% of CO_2 conversion respectively. The catalysts were active at reaction temperature above 200 °C, showing a very high selectivity to methane which close to 100%.and a relatively high stability for 340 h with reduction to about 80% from the initial one.

Previously, Wan Abu Bakar et al., 2010 had investigated Ru/Mn (25:75)/Al_2O_3 which improve catalytic performance. The CO_2 conversion was increased from 17.18% at 200 °C to 89.01% at 400 °C. From the XRD, it can be observed that Mn and Ru enhance the catalytic activity because H_2 and CO_2 are easily chemisorbed and activated on these surfaces. Toemen et al. (2014) also has investigated trimetallic ceria catalyst calcined at 1000 °C with 97.73% CO_2 conversion and 91.31% CH_4 at 200 °C reaction temperature for fuel gases. However, higher based loading and calcination temperature was not cost effective in industrial application.

Therefore, Mat Rosid et al. (2015) has studied Ru/Mn/Ce (5:35:60)/Al_2O_3 catalyst calcined at 700 °C with 100% CO_2 conversion and 80% CH_4 formation. This paper has continued focuses on the optimization of Ru/Mn/Ce (5:35:60)/Al_2O_3 catalyst by Box-Behnken design with three dependable parameter. The optimum condition was studied to improve the catalyst performance during methanation reaction.

2. Experimental

2.1. Preparation of Ru/Mn/Ce(5:35:60)/Al_2O_3 by incipient wetness method

The base metal precursor was prepared by dissolving cerium (III) nitrate hexahydrate (5.00 g) with distilled water and stirred. Then, the manganese nitrate tetrahydrate and ruthenium (III) chloride salt were dissolved with distilled water. These solutions were mixed and stirred continuously by magnetic bar for 30 min at room temperature to homogenize the mixture. Then, alumina beads with diameter of 3 mm was immersed into the catalysts solution for 20 min before transferred onto evaporating dish with glass wool on it. Then the catalyst was aging inside an oven at 80–90 °C for 24 h followed by calcination in the furnace at 400 °C, 600 °C, 700 °C, 800 °C and 1000 °C for 5 h with rate of 10 °C/min.

2.2. Catalytic testing

The catalytic reaction was performed in a fixed micro reactor coupled with Fourier Transform Infrared. The molar ratio reaction gas mixture of CO_2 and H_2 is 1:4 and was passed in heated isothermal tube furnace. A flow rate of $CO_2/H_2 = 50.00$ cm^3/min was used with the increment temperature rate of 5 °C/min.

2.3. Characterization

XRD analysis was conducted by using Diffractometer D5000 Siemens Crystalloflex with CuK_α radiation ($\lambda = 1.54060$ Å). The data obtained was analyzed by a PC interfaced to the diffractometer using software called Diffrac Plus. For FESEM analysis, sample was scanned using Zeiss Supra 35 VP FESEM operating of 15 kV. The catalyst sample was bombarded by electron gun with tungsten filament under 25 kV. N_2 adsorption-desorption isotherms for the catalysts were measured by Micromeritics ASAP 2010. The X-band Bruker electron spin resonance (ESR) spectrometer connected to a Thermo Scientific NESLAB chiller (ThermoFlex3500 model) to control water cooling temperature. The TPR-H_2 and TPD-CO_2 of the catalyst was carried out using Thermo Finnigan TPD/R/O 1100 fitted with a thermo conductivity detector (TCD) and controlled by a computer. The sample was placed in the quartz reactor and was heated from room temperature to 900 °C with heating rate 10 °C/min under a 30 mL/min of 5% H_2 in nitrogen for TPR and a flow of CO_2 (20 mL/min) for TPD analysis.

2.4. RSM for CO_2 methanation optimization over ru/mn/Ce(5:35:60)/Al_2O_3 catalyst

Optimization of Ru/Mn/Ce (5:35:60)/Al_2O_3 for methanation reaction was done using the Design-Expert 7.06 trial (Stat Ease, Inc. Minneapolis, USA). The studied parameters which are calcination temperature (600 °C–800 °C), ratio based loading (60%–80%), and catalyst dosage (3 g- 7 g) and the related parameter effects with response (CO_2 conversion) were analysed and optimized by Box-Behnken design. This parameter was selected based on experimental data obtained during catalytic screening. Fig. 1 showed the flowchart of response surface methodology using Box-Benhken design.

3. Results and discussion

3.1. Characterization

3.1.1. X-rays diffractogram analysis

The changes of phase obtained from XRD analysis for Ru/Mn/Ce (5:35:60)/Al_2O_3 catalyst upon the increase of calcination temperatures are shown in Fig. 2. It was observed that the crystallinity of the catalyst was amended as the calcination temperature increased. This result suggests that crystal lattice has been rearrangement in

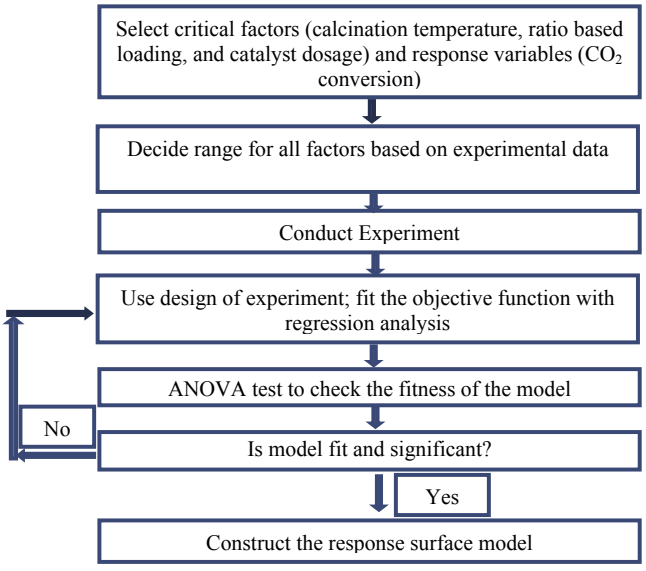

Fig. 1. Flowchart of response surface methodology.

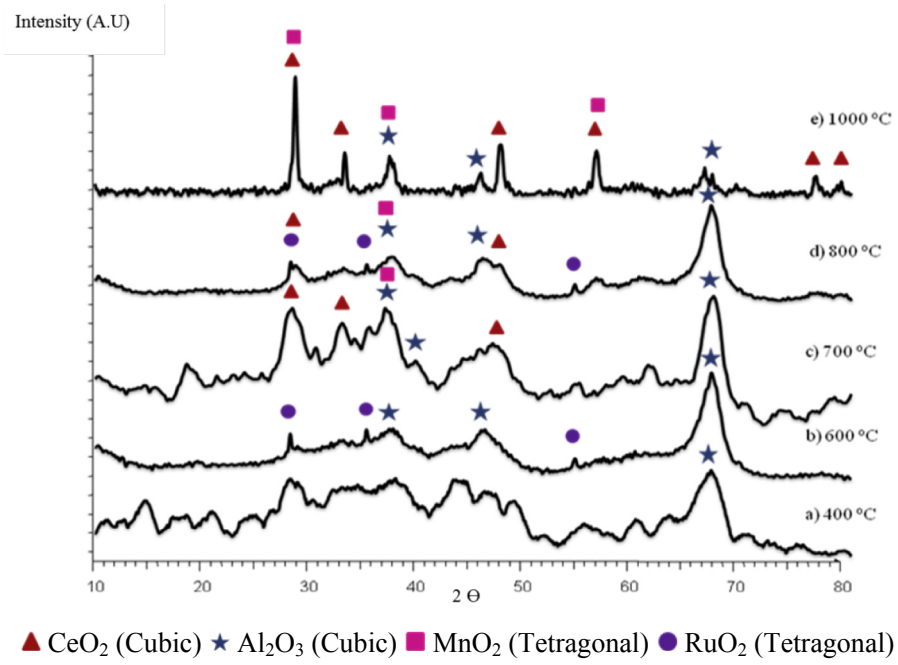

Fig. 2. XRD Diffractograms of Ru/Mn/Ce (5:35:60)/Al_2O_3 catalyst calcined at various temperatures; 400 °C, 600 °C, 700 °C, 800 °C and 1000 °C for 5 h.

order to produce narrow and sharp peaks. Jones et al., 2009 also stated that catalyst calcined at above 500 °C shows high crystallinity. However, in this study, high crystallinity phase was only observed for catalyst calcined at 1000 °C, whereby catalyst calcined at 400 °C showed an amorphous phase and those calcined at 600 °C, 700 °C and 800 °C showed weak crystalline phases. This phenomenon was due to lattice distortion which caused by incorporation of Ce into the catalyst. This is in agreement with Liu et al., 2015, Pal et al., 2012, and Ghosh et al., 2009 who got a similar result when lanthanide element was added to the catalyst.

Diffractogram at 400 °C showed an amorphous and mostly was dominated by the alumina support and no other peak could be assigned. However, when the catalysts were calcined at 600 °C, a peak of Al_2O_3 with cubic phase appeared at 2θ values of 67.23° (I_{100}), 45.26° (I_{45}) and 36.90° (I_{27}). At the same time, a RuO_2 peak (tetragonal phase) was revealed at 2θ values of 28.83° (I_{100}), 45.26° (I_{77}), and 35.70° (I_{77}). Diffractogram of the catalyst calcined at 700 °C showed an increasing intensity with a new peak of CeO_2 (fcc) that were revealed at 2θ values of 28.23° (I_{100}), 47.26° (I_{45}) and 32.90° (I_{27}). Meanwhile, alumina oxide cubic and manganese oxide tetragonal phases were also formed. The distinctive peaks for Al_2O_3 cubic phases were observed at 2θ values of 67.34° (I_{100}), 36.52° (I_{60}), and 39.42° (I_{50}). Manganese oxide with tetragonal phase appeared at 2θ values of 28.23° (I_{100}), and 36.26° (I_{52}). In contrast, the diffractogram calcined at 800 °C exposed a similar pattern with 600 °C which revealed the presence of RuO_2 with tetragonal phase at 2θ values of 28.83° (I_{100}), 45.26° (I_{77}), and 35.70° (I_{77}). Alumina oxide with cubic phase was observed at 2θ values of 67.24° (I_{100}), 45.30° (I_{65}) and 36.72° (I_{60}). Meanwhile, at 1000 °C, the Al_2O_3 cubic phases were detected at 2θ values of 67.13° (I_{100}), 45.60° (I_{100}), and 36.46° (I_{90}) and the peak for cerium oxide with face-centered cubic were assigned at 2θ values of 28.51° (I_{100}), 47.41° (I_{45}), 56.43° (I_{33}), 33.13° (I_{27}), 76.36° (I_{10}) and 79.02° (I_6).

Other than that, in regards to the peaks for manganese oxide, MnO_2 was observed in tetragonal phase and emerged at 2θ values of 28.56° (I_{100}), 36.98° (I_{52}) and 56.60° (I_{48}). The observation is aligned with a study performed by Chun et al. (2011) which stated that when composition of Mn exceeds 0.2 over ratio $Ce_{0.8}/Mn_{0.2}O_2$, the peak assigned to MnO_2 is detected. Xiang and You-chang, 2000 also stated that during the calcination, phase transformation takes place and it crystallizes promptly into large α-Mn_2O_3 particles. However, in the presence of Ce, the crystallization of manganese oxide is strongly impeded, and their surface areas stabilize with MnO_2. The presence of Mn in the host lattice was important as it maintain the substantial activity at high temperature [Tian et al., 2012, Finger et al, 1994]. This is in agreement with Murata et al., 2009 where the existence of Mn species is believed to increase CO_2 conversion by removing Cl atoms from $RuCl_3$ precursor and increases the density of active Ru oxide species on the catalyst. Luo and Li 2004 also stated that the electronegativity of Mn is lower than Ru, however they have similar atomic size which Mn could effectively relax the electron-deficient state of Ru. Therefore, it increased the performance catalytic activity of catalysts in methanation reaction. Besides that, there were overlapping peaks on each other due to phases with distinct but closely related crystallographic characteristics from a complete XRD profile [Xiang and You-chang, 2000].

3.1.2. Electron spin resonance analysis

The g-value at 4.36 was attributed to Al_2O_3 from the support of catalyst. Meanwhile, at g value of 2.12 which exhibited “wing” on both sides was attributed to Mn^{4+} with MnO_2 compound as shown in Fig. 3. This data was supported by Phan et al. (2010) who investigated Mn-doped metal oxide at different calcination temperatures. They stated that MnO_2 exhibited a symmetrical centered at about 300 magnetic field which was caused by a paramagnetic phase. Chakradhar et al, 2000 also stated that the presence of Mn^{2+} or Mn^{3+} did not give any peak in ESR due to low concentration of Mn^{2+} and Mn^{3+} ions. Therefore, it is proven that Ru/Mn/Ce (5:35:60)/Al_2O_3 revealed the presence of Mn^{4+} in XRD analysis which MnO_2 was observed in the diffractogram. The peak of CeO_2 could not be observed due to the diamagnetic properties of Ce^{4+} in the Ru/Mn/Ce (5:35:60)/Al_2O_3 catalyst. The intensity of the peak at 700 °C calcination temperature showed the highest peak among others. Therefore, the strength paramagnetic properties of the catalyst may have been higher at 700 °C, contributing to the highest

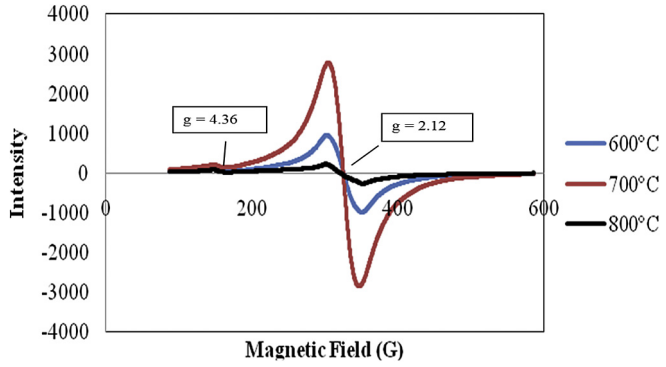

Fig. 3. ESR spectra for Ru/Mn/Ce (5:35:60)/Al_2O_3 catalyst calcined at 600 °C, 700 °C, and 800 °C for 5 h.

catalytic activity of CO_2 conversion. Meanwhile, at 600 °C and 800 °C calcination temperatures, the intensity of peak decreased, implying the decrease in the paramagnetic properties of the catalyst. The ESR signal of the catalysts at all studied calcination temperatures suggesting a tetrahedral symmetry of the paramagnetic Mn ion [Kijlstra et al, 1997]. This is also supported by Christoes et al. (2014) who investigated the structural and magnetic properties of manganese/cerium. They stated that Mn atoms occupy the corners of perfect tetrahedron with Ce at the center. This result is supported with XRD analysis which revealed the presence of tetragonal phase of MnO_2 in the diffractogram and spectra.

3.1.3. Temperature programmed reduction analysis

The H_2-TPR profile for Ru/Mn/Ce (5:35:60)/Al_2O_3 are shown in Fig. 4. At calcination temperature of 600 °C, three reduction peaks were observed at 171.5 °C, 272.6 °C, and 561.9 °C, respectively. The first reduction peak at 171.5 °C was attributed to the reduction temperature for CeO_2-MnO_x which indicates the presence of interaction between manganese and cerium oxide as has been investigated by Gong et al. (2012). The H_2 consumption at first reduction peak was 0.68 cm^3/g STP. The second reduction peak at 272.6 °C was attributed to reduction peak of MnO_2 with H_2 consumption of 3.49 cm^3/g at STP. A similar assignment was made by Gong et al. (2012) on manganese catalyst. Higher H_2 consumption can indicate the turning of several manganese oxide species to higher oxidation states. Meanwhile, the third reduction peak at 561.9 °C was attributed to the reduction of surface cerium, CeO_2 with a total H_2 consumption of 1.05 cm^3/g at STP.

At 700 °C calcination temperature, the first reduction peak in H_2-TPR profile at 276.6 °C with 1.08 cm^3/g at STP of H_2 consumption was attributed to the reduction of MnO_x. For the second reduction peak with 330.5 °C reduction temperature, it was allocated to the reduction of MnO_2 when co-doped with Ce with highest H_2 consumption of 5.51 cm^3/g at STP [Wang et al., 2011]. The third reduction peak at 613.6 °C reduction temperature, with 0.79 cm^3/g at STP can be assigned to the reduction of bulk CeO_2 with easily reducible surface oxygen of the cerium with small crystal size, as supported by FESEM analysis. It was reported that the mobility of oxygen not only occurred in cerium oxides, but also between cerium oxides and supported metal. The similar observation was reported by Zafiris and Gorte (1993). The shifted peaks occur at higher temperature for 700 °C due to strong interaction between metal oxide and support; therefore it needs higher temperature to be reduced as also explained by Dow et al. (2000).

Similar TPR profile with three reduction peaks appeared at temperature of 181.6 °C, 293.9 °C, and 652.1 °C was observed on catalyst calcined at 800 °C. The first reduction peak was attributed to the reduction of CeO_2-MnO_x which showed a shift to higher regions, indicating a stronger interaction between manganese and cerium oxides (Gong et al. (2012)) as compared to when calcined at 600 °C. The H_2 consumption for the first reduction peak was 0.68 cm^3/g at STP. The second reduction peak was attributed to the reduction of MnO_2 as discussed earlier for the catalyst at 600 °C calcination temperature. Meanwhile, the third reduction peak was ascribed to the reduction of surface and bulk oxygen of CeO_2 (Holgado et al. (2000)) with H_2 consumption was 0.78 cm^3/g STP. From the TPR profile, no reduction peak of γ-Al_2O_3 was observed, proving that γ-Al_2O_3 is an inert support.

3.1.4. Temperature programmed desorption analysis

Temperature programmed desorption analysis was conducted to determine the sorption profile of CO_2 and H_2 on the surface of catalyst as well as to measure the basicity of the catalyst surface. TPD profile of CO_2 for Ru/Mn/Ce (5:35:60)/Al_2O_3 is shown in Fig. 5.

CO_2-TPD profile revealed two profound desorption peaks around 105.6 °C and 208.3 °C which can be distinguished. The first and second peaks were assigned to CO adsorbed on the manganese species [Wang et al. (2011)]. The area for the second peak was much larger, implying that more manganese active sites were present as CO adsorption sites in Ru/Mn/Ce (5:35:60)/Al_2O_3. The second peak also showed a level of intensity which was a little higher, indicating that more manganese species were present as CO adsorption sites on its surface. The coordination of CO_2 onto metal oxide has different energies which causes different desorption profiles. The lowest desorption temperature was due to desorption of the weakest bonding mode of CO_2 onto the catalyst surface. The area under TPD profile is a measure of the total acidity of the catalyst.

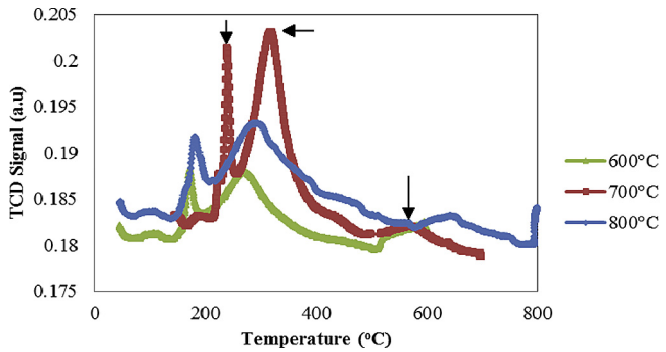

Fig. 4. H_2-TPR profile of Ru/Mn/Ce (5:35:60)/Al_2O_3 at different calcination temperatures.

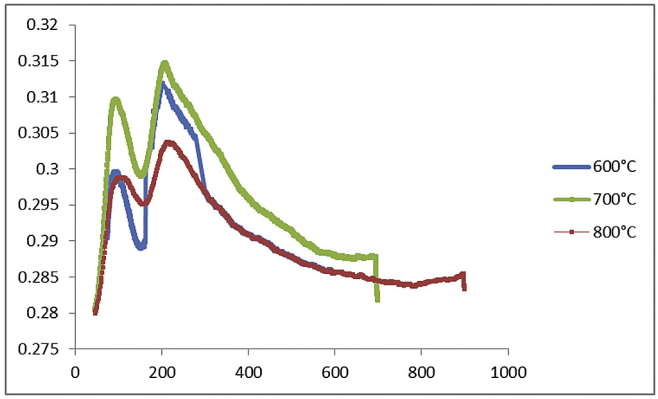

Fig. 5. CO_2-TPD curve over Ru/Mn/Ce (5:35:60)/Al_2O_3 catalyst calcined at 600 °C, 700 °C and 800 °C for 5 h.

The broad peak area around 208.3 °C indicated higher basicity surface of catalyst due to the many CO_2 desorbed on the basic sites of catalyst [Wang et al. (2011)]. Therefore, higher intensity of peak at 700 °C indicated of increasing the catalytic activity of the catalyst compared to other calcination temperature.

3.1.5. Field emission scanning electron microscopy (FESEM) analysis

Fig. 6 shows the FESEM micrographs of Ru/Mn/Ce (5:35:60)/Al_2O_3 catalyst calcined at 400 °C, 600 °C, 700 °C, 800 °C and 1000 °C for 5 h. The magnification used was 50000×. The morphology of cerium oxide catalyst showed a significant difference when subjected to various calcination temperatures. As can be observed, the particle size became larger when the calcination temperature was increased. This can be supported by XRD analysis which revealed the crystallinity of the peak increased when calcination temperatures also increased as indication of particle size became larger. However, at 1000 °C calcination temperature, the micrograph showed a good dispersion of surface catalyst with spherical shape of uncertain sizes. This was supported by Nurunnabi et al. (2008) that stated the moderate particle size and pore diameter of the catalyst is an important for the higher CO_2 conversion. At 800 °C calcination temperature, the catalyst surface was densely packed, which consequently lowered the surface area of the catalyst sample. Densely packed surface of catalyst will reduce surface area of the catalyst thus decreasing the catalytic activity performance. The morphology was supported with XRD which revealed the amorphous phase at 400 °C–800 °C calcination temperature. However, at 1000 °C calcination temperature, XRD analysis showed a crystalline peak with bigger particle size in micrograph.

3.1.6. Nitrogen adsorption analysis

Table 1 summarizes the textural analysis of Ru/Mn/Ce (5:35:60)/Al_2O_3 catalyst with various calcination temperatures of 400 °C, 600 °C, 700 °C, 800 °C and 1000 °C. Specific surface area is one of the important parameter in heterogeneous catalyst. From Table 1, the BET surface area for Ru/Mn/Ce (5:35:60)/Al_2O_3 catalysts decreases as the calcination temperature was increased. It is suggested that the relative reduction of BET surface area for the catalyst at high calcination temperature was attributed to the shrinkage and agglomeration of metallic oxide particles when calcined at higher temperature. This may have been due to the decrease of surface area and larger pores which resulted in sintering that lead to a loss in activity of the catalyst due to the pore elimination and formation of dense solid [Contreras *et al,* 2009]. Hence, it can be concluded that high surface area is important in performing high catalytic activity catalyst as it provides more active surface to catalyse the reaction. Average pore diameter increased when calcination temperature was increased. This is due to the packing effect that leads to the difference in maximum density in each pore.

3.2. Catalytic activity testing

3.2.1. Effect of calcination temperature

The catalysts were subjected to calcination temperatures of 400 °C, 600 °C, 700 °C, 800 °C, 900 °C, 1000 °C, and 1100 °C for Ru/Mn/Ce (5:35:60)/Al_2O_3. Fig. 7 shows the trend of catalytic activity for all the potential catalysts from FTIR analysis. From the figure, it can be observed that when calcination temperature was increased from 400 °C to 700 °C, the CO_2 conversion increased accordingly.

At 400 °C, the CO_2 conversion was 92%, followed by 600 °C with 85% and 700 °C with 100% of catalytic activity. From 800 °C to 1100 °C calcination temperature, the CO_2 conversion decreased. This is possibly due to the enlargement of the particle size through agglomeration process as the calcination temperature was increased. Therefore, it could be concluded that calcination temperature of 700 °C was the best calcination temperature as it gave

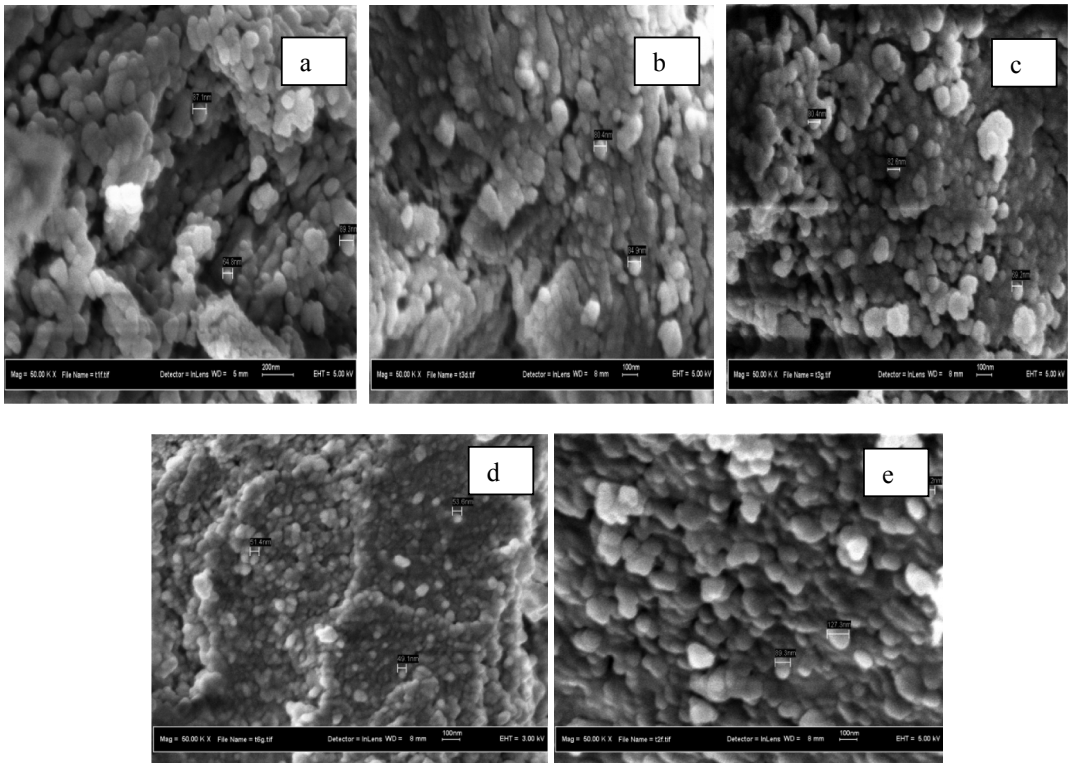

Fig. 6. FESEM micrographs of Ru/Mn/Ce (5:35:60)/Al_2O_3 catalyst calcined at a) 400 °C, b) 600 °C, c) 700 °C, d) 800 °C, and e) 1000 °C for 5 h in 50000x magnification, scale bar: 100 μm.

Table 1
Textural analysis of Ru/Mn/Ce (5:35:60)/Al_2O_3 catalyst at different calcination temperatures.

Catalyst	Calcination Temperature, °C	S_{BET} (m^2/g)	Average Pore Diameter (nm)	Pore Volume (cm^3/g)
Ru/Mn/Ce (5:35:60)/Al_2O_3	400	224.29	56.23	0.30
	600	167.19	77.23	0.32
	700	143.10	99.15	0.34
	800	132.78	111.12	0.37
	1000	50.95	164.92	0.36

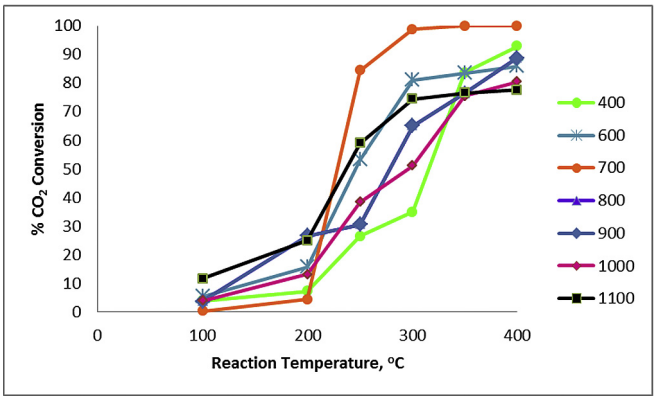

Fig. 7. CO_2 conversion of Ru/Mn/Ce (5:35:60)/Al_2O_3catalyst calcined at various calcination temperatures for 5 h, 7 g catalyst.

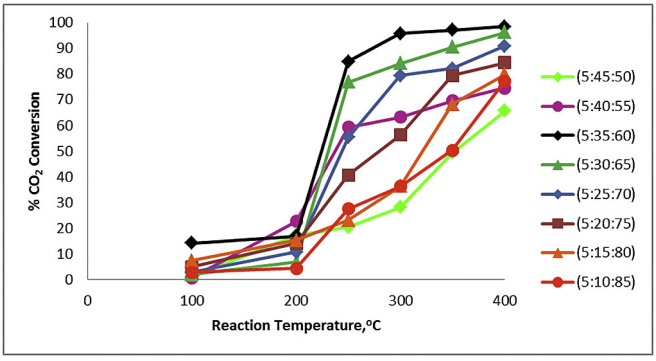

Fig. 8. CO_2 conversion of Ru/Mn/Ce/Al_2O_3 catalyst calcined at 700 °C for 5 h with various metal oxide based loadings with 7 g catalyst dosage.

the highest catalytic activity with 100% of CO_2 conversion at 350 °C reaction temperature as supported by TPD analysis (Fig. 5) which showed a higher intensity of basicity site at that temperature.

At 800 °C–1100 °C, the CO_2 conversion was slightly decreased from the previous catalyst which may have been due to agglomeration of particles, thus resulting in the formation of larger crystallite as discussed by Sehested (2003). This is supported with BET analysis which showed a decreasing of surface area when the calcination temperature was increased (Refer Table 1). During calcination also, some of the smaller CeO_2 particles may also be broken down and saturate the dispersed phase while other CeO_2 particles coalesce and grow larger, contributing to the decrease of catalytic activity at 800 °C–1100 °C [Schmitz et al, 1993].

3.2.2. Effect of cerium oxide based loadings

The potential catalysts were optimized by using various cerium based loadings in order to observe the effect on the catalytic performance. All the prepared catalysts showed lower performances at low reaction temperature; however it started to increase drastically from reaction temperature of 250 °C–400 °C as depicted in Fig. 8. From the CO_2 conversion obtained, Ru/Mn/Ce/Al_2O_3 with ratio 5:35:60 was assigned as the best catalyst with 100% of CO_2 conversion at 350 °C reaction temperature and selected to be the optimum ratios.

From the figure, the CO_2 conversion was increased when the Ce loading was increased to 60%, but decreased as the Ce content was increased up to 85%. This phenomenon was due to hindrance of the active sites by disproportionate loading of Ce. This result was similar with He et al. (2011) who stated that with the increase of Ce content, it is capable of promoting a particle to agglomerate thus, retarded the growth of crystal size which would then cause a blockage of the surface of the active site. Perkas et al. (2009) also stated that the lowest activity of catalyst occurred with the presence of the largest amount of Ce loadings because the blocking of the pores structure could result in preventing of the activation of the reagents. The trend plots of catalytic performance are shown in Fig. 8.

3.2.3. Effect of catalyst loading

Optimization parameter with different loading of catalyst during reaction was also investigated in this study. At reaction temperature 250 °C, the CO_2 conversion for each catalyst dosage started to increase drastically. The highest CO_2 conversion was achieved with 7 g of catalyst dosage. From Fig. 9, it can be observed that when the catalyst dosage was increased, the catalytic CO_2 conversion also increased. This may be due to the increase of active site with the increased of catalyst loading. This is in agreement with Su et al (2010) who stated that the effectiveness of the catalytic activity showed an increase which was parallel to the increase of catalyst dosage. Therefore, the trend of catalyst dosage towards highest CO_2 conversion was 3 g $<$ 5 g $<$ 7 g. Fig. 9 depicts the trend plot of the catalyst dosage.

3.2.4. Effect of CO_2 ratio

The molar ratio CO_2 in the CO_2/H_2 mixture has been optimized up to 4% of CO_2 in the feed system before passing through the catalyst. For the crude natural gas, the CO_2 contents can vary from 4 to 50% depending on gas source [Ahmad et al., 2010]. Therefore, the molar ratio of CO_2/H_2 mixture in simulated natural gas has been

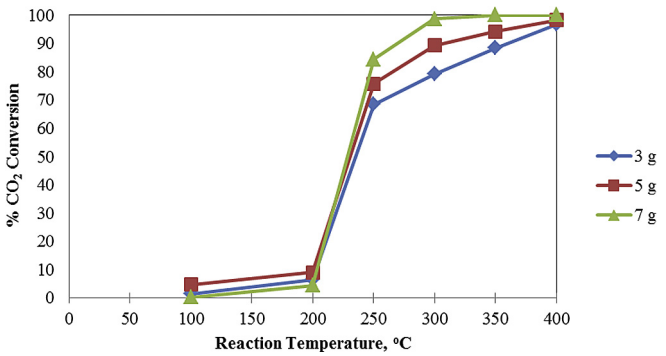

Fig. 9. CO_2 conversion of Ru/Mn/Ce (5:35:60)/Al_2O_3 catalyst calcined at 700 °C for 5 h with various catalyst loadings.

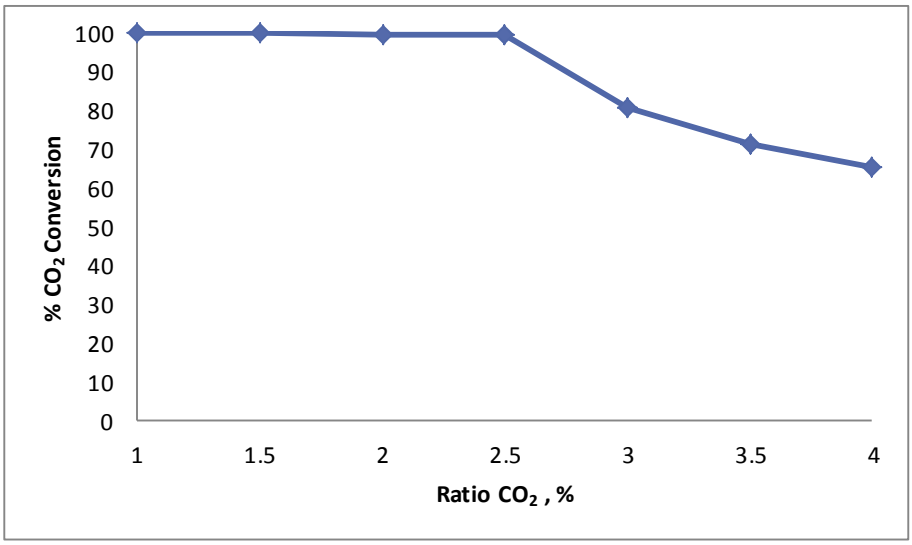

Fig. 10. CO_2 conversion for various molar ratios of CO_2 gas in the CO_2/H_2 mixture in methanation reaction.

investigated up to 4 which are similar to 80% of CO_2 content in crude natural gas. From Fig. 10, it can be observed that when the molar ratio of CO_2 is higher, the CO_2 conversion is slightly decreased which might due to unproportionate amount of H_2 to react with CO_2 gas to form product CH_4 gas [Ismail, 2009].

3.3. Statistical analysis

The parameters for response surface studied were calcination temperature (600 °C–800 °C), Ratio (60%–80%), and catalyst dosage (3 g–7 g). The experimental design was conducted out based on results obtained in the preliminary study. Polynomial regression modelling was conducted between dependent variable and three independent variables as depicted in Table 2. The model equation obtained from the statistical analysis was used to modify the regression model accuracy as shown in an equation below which A is calcination temperature, B is ratio of base and C is catalyst dosage:

$$CO_2\ \text{conversion} = +94.32 - 2.12A - 3.49B + 0.85C - 0.38AB - 0.21AC - 0.90BC - 9.03A^2 + 0.18B^2 + 0.75C^2 \quad (1)$$

This model can be used to predict the CO_2 conversion within the expected experimental data. The adequate of this model was confirmed by the coefficient of determination, R^2 and adjusted R^2, and it should be at least 0.80 for a preferable fit of a model and approximate to the value of one is desired. The value predicted R^2 is in reasonable agreement with the adjusted R^2 representing that the sample size and the number of terms in the model are rational and acceptable. Adequate precision must be greater than 4 to give an adequate model which is important to compares the range of the predicted values at the design points to the average prediction error. For this study, the R^2 value was 0.9514, which means that predicted and actual CO_2 conversion are accordance.

3.3.1. Optimization and model validation (confirmation test)

To validate the optimum conditions to maximize the CO_2 conversion, Design Expert software was operated by setting the goal selection of each arguments (calcination temperature, ratio, and dosage catalyst) "in range", response (% CO_2 conversion) being "in target" which reveal as follows: calcination temperature of 697.47 °C, ratio of 60.38% and dosage catalyst 6.94 g. At these condition, the result was confirmed and verified experimentally

Table 2
Experimental design for CO_2 conversion and results response.

Run	Calcination Temperature A (°C)	Ratio B (%)	Catalyst Dosage C (g)	CO_2 Conversion (%)	
				Actual	Predicted
1	800	60	5	87.20	86.52
2	600	70	7	90.20	89.54
3	800	70	5	83.76	84.23
4	600	80	7	96.30	96.54
5	700	70	5	95.00	94.34
6	700	60	7	100.00	100.00
7	600	70	3	87.89	87.42
8	800	80	5	80.00	79.55
9	600	60	5	90.20	90.85
10	800	70	3	82.30	82.96
11	600	80	5	83.20	84.98
12	700	60	5	94.00	96.87
13	700	80	7	92.00	91.28
14	700	70	3	97.60	95.34
15	700	80	3	92.30	92.09
16	700	80	5	92.00	93.58
17	700	60	3	96.70	96.72

Table 3
ANOVA summarization for response surface model (response: CO_2 Conversion).

Source	Sum of Squares	Mean Square	F value	p-Value Prob>F
Model	484.32	54.08	12.59	0.0015[a]
A-Calcination Temp	35.83	35.83	8.34	0.0234
B-Ratio	97.30	97.30	22.64	0.0021
C-Catalyst Dosage	5.73	5.73	1.33	0.2861
Residual	30.08	4.30		
Lack of Fit	2.74	0.91	0.17	0.9139[b]
Std Dev	1.88	R^2	**0.9514**	
Mean	90.51	Adj R^2	0.8889	
CV	2.08	Pred R^2	0.8464	
PRESS	78.21	Adeq Precision	14.333	

[a] Significant.
[b] Not significant.

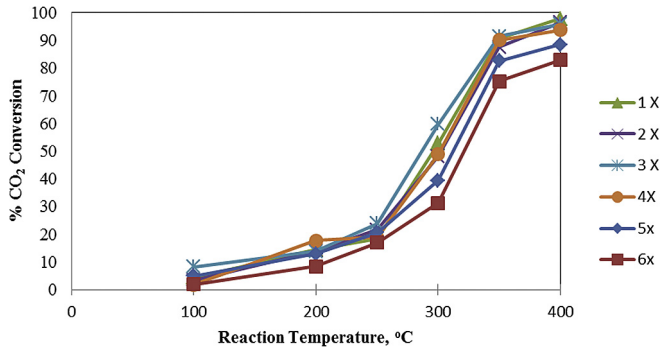

Fig. 11. Reproducibility test of Ru/Mn/Ce (5:35:60)/Al_2O_3 catalyst calcined at 700 °C for 5 h with 7 g catalyst dosage.

(99.98% CO_2 conversion), which was very close to the predicted value with 100% CO_2 conversion.

3.4. Reproducibility test

Reproducibility test was carried out using Ru/Mn/Ce (5:35:60)/Al_2O_3 catalyst several times until the catalytic performance was decreased. Fig. 11 depicts the trend of reproducibility test for Ru/Mn/Ce (5:35:60)/Al_2O_3 catalyst after 6 times of reuse before it deactivated to lower CO_2 conversion. The figure showed that each time tested catalysts were run, a similar pattern with gradual increase of CO_2 conversion up to 250 °C reaction temperature was obtained. However, the catalytic CO_2 conversion showed a drastic increase until maximum studied reaction temperature. The activity was unchanged up to 4 times of reactions. However, at the fifth reaction run, the CO_2 conversion started to slightly decline and continued to decrease up to 80% of CO_2 conversion at 400 °C reaction temperature for 6X times used. According to the study conducted by Bartholomew (2011), deactivation of catalyst might occur due to thermal degradation of active phase crystallite growth which caused a collapse of the pore structure of support at high temperature.

3.5. Stability test

Stability testing was conducted on stream continuously for 7 h at 300 °C reaction temperature, as shown in Fig. 12. The Ru/Mn/Ce(5:30:65)/Al_2O_3 catalyst continued to show a good level of stability with a CO_2 conversion above 90% for 7 h reaction time without drastic decline. The catalytic performance of Ru/Mn/Ce(5:30:65)/Al_2O_3 catalyst was maintained for 2 h and started to decrease slightly to 90% during the reaction time. It shows that the stability of the catalyst during the reaction was might due to addition of manganese and ruthenium. As investigated by Radu (1998), manganese oxide has a characteristic berthollide structure

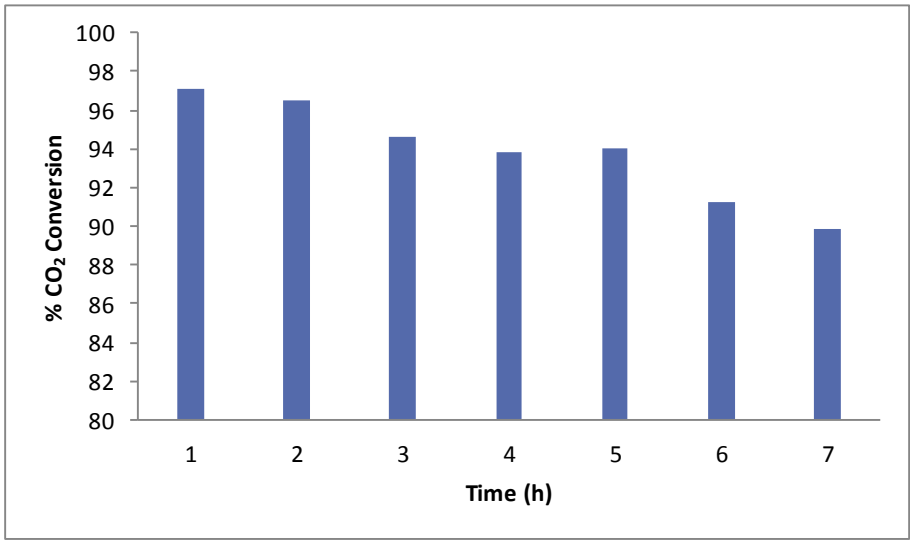

Fig. 12. Stability test on Ru/Mn/Ce (5:35:60)/Al_2O_3 catalyst at 350 °C reaction temperature.

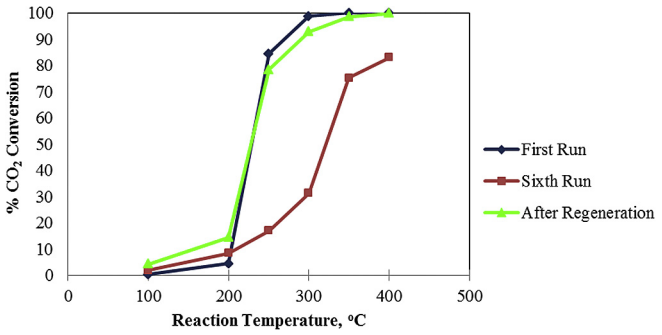

Fig. 13. Regeneration test on Ru/Mn/Ce (5:35:60)/Al_2O_3 catalyst at 700 °C calcination temperature.

that contains labile lattice oxygen storage capacity in crystalline structure. Therefore, the Mn significantly influences its bulk and surface structure with the support and other components present in the catalyst. This is supported with Zhao et al. (2012) who found that incorporation of manganese have led to the formation of an exceedingly stable catalyst.

3.6. Regeneration test

Regeneration test was conducted to determine the reusability of the catalyst. The deactivated catalyst from Section 3.4 was used to perform this phase of the study. Fig. 13 shows the trend plot of regenerated catalyst testing of Ru/Mn/Ce (5:35:60)/Al_2O_3 catalyst. In this study, the regeneration process was conducted in oxidative condition due to the waste catalyst being exposed to the oxygen, as also investigated by Furimsky and Massoth (1993). The compressed air was used to flush the impurities on the catalyst surface by heating it at 100 °C for1 hour in the flow of compressed air. The carbon deposition problem was avoided by adding hydrogen gas flow through the feed stream so that a kinetic or themodynamic equilibra were unfavourable towards the deactivation, as also mentioned by Gardner and Bartholomew (1981).

Approximately almost 100% of recovery was achieved at 400 °C reaction temperature. The catalytic activity showed a slight increase from 100 °C to 200 °C reaction temperature. Alternatively, at 250 °C–350 °C reaction temperature, the CO_2 conversion was slightly lower compared to the fresh catalyst. This phenomenon may have been due to the incomplete removal of impurities from the surface of catalyst at low heating temperature. This finding is supported by Henni and Herman (1991) who found that the regeneration of deactivated catalyst with an oxygen gas was rather prefer carried out at temperature range of 300 °C-550 °C.

4. Conclusion

The effects of three variables; calcination temperature, ratio and catalyst dosage on Ru/Mn/Ce (5:35:60)/Al_2O_3 for CO_2 conversion were studied by conducting Box-Behnken experimental design and RSM. The ANOVA revealed that based ratio is the most significant factor influencing the response variables (CO_2 conversion). Additionally, the calcination temperature provided secondary contribution followed by dosage catalyst to the responses investigated. The quadratic models developed using Box-Behnken design were reasonably acceptable and can be used for prediction within the limits of the factors due to high coefficient of determination value R^2 of 0.9514. The optimum conditions calculated by the regression equation were 700 °C calcination temperature, 70% ratio and 5 g at the point 94% of CO_2 conversion, which fixed well to the expected value. The suggested optimum parameters also showed the presence of active species which are Ce^{4+} and Mn^{4+} as observed in ESR analysis and exhibited the highest surface area with higher intensity of basicity site as observed from TPD analysis. This study verified that Box-Behnken design with response surface methodology could efficiently be applied for modelling catalytic activity of methanation reaction. This designs also one of economical way in obtaining the information in a short period of time with the fewest number of experiments.

Acknowledgement

Foundation items: Universiti Teknologi Malaysia and Ministry of Higher Education (MOHE), Malaysia for the financial support given under the GUP, Vot 13H34 and Professional Development Research University (PDRU) grant vote 03E38 given to Salmiah Jamal binti Mat Rosid.

References

Ahmad, F., Lau, K.K., Shariff, A.M., 2010. Removal of CO_2 from natural gas using membrane separation systems: modelling and process design. J. Appl. Sci. 10 (12), 1134–1139.
Bartholomew, C.H., 2011. Carbon deposition in stream reforming and methanation. Appl. Catal. A General 212, 17–60.
Biinzli, J.-C.G., Piguet, C., 2005. Taking advantage of luminescent lanthanide ions. Chem. Soc. Rev. 34, 1048–1077.
Chakradhar, P.S., Murali, A., Rao, J.L., 2000. A study of electron paramagnetic resonance and optical absorption in calcium manganese phosphate glasses containing praseodymium. J. Mater. Sci. 35, 353–359.
Christoes, L., Annaliese, E.T., Kylie, J.M., Khalil, A.A., George, C., 2014. Manganese/cerium clusters spanning a range of oxidation levels and $CeMn_8$, Ce_2Mn_4, and Ce_6Mn_4 Nuclearities: structural, magnetic, and EPR properties. Inorg. Chem. 53, 6805–6816.
Chun, T.P., Hsing, K.L., Biing, J.L., Yin, Z.C., 2011. Removal of CO in excess hydrogen over CuO/$Ce_{1-x}Mn_xO_2$ catalyst. Chem. Eng. J. 172, 452–458.
Contreras, J.L., Fuentes, G.A., Zeifert, B., Salmones, 2009. Stabilization of supported platinum nanoparticles on γ-alumina catalysts by addition of tungsten. J. Alloys Compd. 483 (1–2), 371–373.
Dong, X., Pi, G., Ma, Z., Dong, L., 2017. The perform of the natural gas industry in the PR of China. Renew. Sustain. Energy Rev. 73, 582–593.
Dow, W.P., Wang, Y.P., Huang, T.J., 2000. TPR and XRD studies of yttria-doped ceria/γ-alumina supported copper oxide catalyst. Appl. Catal. A General 190, 25–34.
Du, G., Lim, S., Yang, Y., Wang, C., Pfefferle, L., Haller, G.L., 2007. Methanation of carbon dioxide on Ni-incorporated MCM-41 catalysts: the influence of catalyst pretreatment and study of steady state reaction. J. Catal. 249, 370–379.
Finger, L.W., Cox, O.E., Jephcoat, A.P., 1994. A correction for powder diffraction peak symmetry due to axial divergence. J. Appl. Cryst 27 (6), 892–900.
Furimsky, E., Massoth, F.E., 1993. Introduction of regeneration of hydroprocessing catalysts. Catal. Today 17 (4), 537–659.
Gardner, D.C., Bartholomew, C.H., 1981. Kinetics of carbon deposition during methanation of CO. Ind. Eng. Chem. Prod. Res. Dev. 20 (1), 80–87.
Ghosh, P., La Rosa, E., Oliva, J., Solis, D., Kar, A., Patra, A., 2009. Influence of surface coating on the upconversion emission properties of $LaPO_4$:Yb/TmLaPO$_4$:Yb/Tm core-shell nanorods. J. Appl. Phys. 105, 113532.
Gong, L., Luo, L.T., Wang, R., Zhang, W., 2012. Effect of preparation methods of CeO_2-MnO_x mixed oxides on preferential oxidation of CO in H_2-rich gases over CuO-based catalysts. J. Chil. Chem. Soc. 57, 1048–1053.
He, H.Q., Zhang, L., Wu, H., Li, C.Z., Jig, S.P., 2011. Synthesis and characterization of doped $La_9ASi_6O_{26.5}$ (A= Ca,Sr,Ba) oxy apatite electrolyte by water-based gel-casting route. Int. J. Hydrogen Energy 36 (11), 6862–6874.
Henni, S., Herman, K.W., 1991. Method for the Regeneration of Spent Alumina-based Catalysts. European Patent 0244014B1. Retrieved on August 21, 1991. http://www.yellowpages.com.my/energyguide/.
Holgado, J.P., Alvarez, R., Munvera, G., 2000. Study of CeO_2, XPS spectra by factor analysis: reduction of CeO_2. Appl. Surf. Sci. 161, 301–315.
Islam, M.R., Saidur, R., Rahim, N.A., Solangi, K.H., 2009. Renewable energy Research in Malaysia. Eng. e-Trans. 4 (2), 69–72.
Ismail, A.F., 2009. Specialized Workshop on Membrane Gas Separation Technology. Advanced Membrane Technology Research Centre, Malaysia.
Jones, C., Cole, K.J., Taylor, S.H., Crodace, M.J., Hutchings, G.J., 2009. Copper manganese oxide catalysts for ambient temperature carbon monoxide oxidation: effect of calcination on activity. J. Mol. Catal. A Chem. 305 (1–2), 121–124.
Kakaee, A.-H., Paykani, A., Ghajar, M., 2014. The influence of fuel composition on the combustion and emission characteristics of natural gas fueled engines. Renew. Sustain. Energy Rev. 38, 64–78.
Kijlstra, W.S., Poels, E.K., Blick, A., 1997. Characterization of Al_2O_3 supported manganese oxide by electron spin resonance and diffuse reflectance spectroscopy. J. Phys. Chem. B 101, 309–316.
Liu, X., Deng, R., Zhang, Y., Wang, Y., Chang, H., Huang, L., Liu, X., 2015. Probing the

nature of up conversion nanocrystals: instrumentation matters. Chem. Soc. Rev. 44, 1479–1508.
Luo, L., Li, S., 2004. Effect of transition metals on catalytic performance of Ru/Sepolite catalyst for methanation of carbon dioxide. J. Nat. gas Chem. 13, 45–48.
Mat Rosid, S.J., Wan Abu Bakar, W.A., Ali, R., 2015. Catalytic CO_2/H_2 methanation reaction over alumina supported manganese/cerium oxide based catalysts. Adv. Mater. Res. 1107, 67–72.
Murata, K., Okabe, K., Inaba, M., Takahara, I., Liu, Y., 2009. Mn-modified Ru catalysts supported on carbon nanotubes for Fisher Tropsch synthesis. J. Jpn. Petrol. Inst. 52 (1), 16–20.
Nurunnabi, M., Murata, K., Okabe, K., Inaba, M., Takahara, I., 2008. Performance and characterization of Ru/Al_2O_3 and Ru/SiO_2 catalysts modified with Mn for Fischer–Tropsch synthesis. Appl. Catal. A General 340, 203–211.
Osazuwa, O.U., Cheng, C.K., 2017. Catalytic conversion of methane and carbon dioxide (greenhouse gases) into syngas over samarium-cobalt-trioxides perovskite catalyst. J. Clean. Prod. 148, 202–211.
Pal, M., Pal, U., Miguel, J., Jimenez, G.Y., Perez-Redriguez, F., 2012. Effect of crystallization and dopant concentration on the emission behaviour of TiO2:Eu nanophosphorous. Nanoscale Res. Lett. 7 (1), 1–12.
Pan, S.-Y., Wang, P., Chen, Q., Jiang, W., Chu, Y.-H., Chiang, P.-C., 2017. Development of high gravity technology for removing particulate and gaseous pollutant emissions: principle and applications. J. Clean. Prod. 149, 540–556.
Perkas, N., Amirian, G., Zhong, Z., Teo, J., Gofer, Y., Gedanken, A., 2009. Methanation of carbon dioxide on Ni catalysts on mesoporous ZrO_2 doped with rare earth Oxides. Catal. Lett. 130, 455–462.
Phan, T.L., Zhang, P., Tran, H.D., Yu, S.C., 2010. Electron spin resonance study of Mn-doped metal oxides annealed at different temperatures. J. Korean Phys. Soc. 57 (5), 1270–1276.
Radu, C., 1998. Strucrure/activity correlation for unpromoted and CeO_2-promoted MnO_2/SiO_2 catalyst. Catal. Lett. 55, 25–31.
Rao, G.R., Mishra, B.G., 2003. Structural, redox and catalytic chemistry of ceria based materials. Bull. Catal. Soc. India 2, 122–134.
Sadegh, N., Stenby, E.H., Thomsen, K., 2017. Thermodynamic modelling of acid gas removal from natural gas using the extended UNIQUAC model. Fluid Phase Equilibria 442, 38–43.
Schmitz, P.J., Usmen, R.K., Poters, C.R., Graham, G.W., Mc Case, R.W., 1993. Effect of calcination temperature on Al_2O_3-supported CeO_2: complementary from XRD and XPS. Appl. Surf. Sci. 72, 181–187.
Sehested, J., 2003. Sintering of steam reforming catalysts. J. Catal. 217 (2), 417–426.
Su, P., Chu, O., Wang, L., 2010. Studies on catalytic activity of nanostructure Mn_2O_3 prepared by solvent-thermal method on degrading crystal violet. Mod. Appl. Sci. 4 (5), 125–129.
Tian, G., Gu, Z.J., Zhou, L.J., Yin, W.Y., Liu, X.X., Yan, L., Jin, S., Ren, W.L., Xing, G.M., Li, S.J., Zhou, Y.L., 2012. Mn^{2+} dopant-controlled synthesis of $NaYF_4$:Yb/Er upconversion nanoparticles for in vivo imaging and drug delivery. Adv. Mater 24, 1226–1231.
Toemen, S., Bakar, W.A.W.A., Ali, R., 2017. CO_2/H_2 methanation technology of strontia based catalyst: physicochemical and optimisation studies by Box–Behnken design. J. Clean. Prod. 146, 71–82.
Toemen, S., Wan Abu Bakar, W.A., Ali, R., 2014. Investigation of $Ru/Mn/Ce/Al_2O_3$ catalyst for carbon dioxide methanation: catalytic optimization, physicochemical studies and RSM. J. Taiwan Inst. Chem. Eng. 45, 2370–2378.
Wan Abu Bakar, W.A., Ali, R., Sulaiman, N., Abdul Rahim, H.F., 2010. Manganese oxide doped noble metals supported catalyst for carbon dioxide methanation reaction. Trans. C Chem. Chem. Eng. Sci. Iran. 17, 115–123.
Wang, Z., Li, X., Song, W., Chen, J., Li, T., Feng, Z.P., 2011. Synergetic promotional effects between cerium oxide and manganese oxides for NH_3 selective catalyst reduction over Ce-Mn/TiO_2. Mater. Express 1 (2), 167–175.
Xiang, W., You-chang, X., 2000. Total oxidation of methane over La, Ce and Y Modified manganese oxide catalysts. React. Kinet. Catal. Lett. 71 (1), 3–11.
Zafiris, G.S., Gorte, R.J., 1993. Evidence for a second CO oxidation mechanism on Rh/ceria. J. Catal. 139, 561.
Zhang, Y., Liu, Q., Zhou, Y.D., Ying, B., 2017. Integrated optimization of cutting parameters and scheduling for reducing carbon emissions. J. Clean. Prod. 149, 886–895.
Zhao, A., Ying, W., Zhang, H., Hongfang, M., Fang, D., 2012. Ni/Al2O3 catalysts for syngas methanation: effect of Mn promoter. J. Nat. Gas Chem. 2, 170–177.